Liquid Crystals
Publication details, including instructions for authors and subscription information:
http://www.informaworld.com/smpp/title~content=t713926090

Substitution effects on the liquid crystalline properties of D,L-xylitol amphiphiles

John W. Goodby; Julie A. Haley; Marcus J. Watson; Grahame Mackenzie; Stephen M. Kelly; Philippe Letellier; Olivier Douillet; Paul Gode; Gerard Goethals; Gino Ronco; Pierre Villa

Online publication date: 29 June 2010

To cite this Article Goodby, John W. , Haley, Julie A. , Watson, Marcus J. , Mackenzie, Grahame , Kelly, Stephen M. , Letellier, Philippe , Douillet, Olivier , Gode, Paul , Goethals, Gerard , Ronco, Gino and Villa, Pierre(1997) 'Substitution effects on the liquid crystalline properties of D,L-xylitol amphiphiles', Liquid Crystals, 22: 3, 367 — 378
To link to this Article: DOI: 10.1080/026782997209441
URL: http://dx.doi.org/10.1080/026782997209441

LIQUID CRYSTALS, 1997, VOL. 22, NO. 3, 367–378

Substitution effects on the liquid crystalline properties of D,L-xylitol amphiphiles

by JOHN W. GOODBY*, JULIE A. HALEY, MARCUS J. WATSON, GRAHAME MACKENZIE, STEPHEN M. KELLY, PHILIPPE LETELLIER
The School of Chemistry, The University of Hull, Hull HU6 7RX, England

OLIVIER DOUILLET, PAUL GODÉ, GERARD GOETHALS, GINO RONCO, and PIERRE VILLA
Université de Picardie, Jules Verne, Faculté des Sciences, Laboratoire de Chimie Organique et Cinétique, 33 rue Saint Leu—80039, Amiens CEDEX, France

(*Received 31 July 1996 and accepted 24 October 1996*)

In this article we describe the self-assembling properties of alkyl substituted xylitols in relation to both thermotropic and lyotropic liquid crystalline mesophases. Three series of substituted xylitols were prepared where aliphatic chains of varying length were attached to a xylitol moiety via ether, thioether and ester linking groups. The thermotropic properties were investigated by thermal polarized light microscopy and differential scanning calorimetry, and evaluated as a function of chain length and linking group. The lyotropic phase behaviour was investigated via the addition of water to each material at room temperature. The efficiency for forming thermotropic phases was found to be reversed for the lyotropic phases in respect of the three series, i.e. as a function of the linking unit.

1. Introduction

In 1983 Jeffrey and Bhattacharjee showed that a variety of *n*-alkyl substituted glucopyranosides exhibited thermotropic liquid crystalline properties [1]; this result concurred with earlier speculations that many biologically active materials, e.g. DNA, phosphatidyl cholines and ethanolamines, cholesterol derivatives, etc., could exhibit both lyotropic and thermotropic liquid crystalline properties [2, 3].

The thermotropic mesophase exhibited by the alkyl 1-*O*-*β*-D-glucopyranosides was classified as being essentially smectic A* in type [4]. In addition, it was suggested that clusters or associations of the molecules via hydrogen bonding were instrumental in the stabilization of the structure of the mesophase, and a simple bilayer model of the structure of the smectic A* phase was proposed to explain this phenomenon [4]. In this structural model the molecular layers are held together by hydrogen bonding of the carbohydrate moieties along the median of the layers. The liquid-like aliphatic chains then form the outer regions of the layers; thus the model is comparable to the typical bilayer structure found in conventional thermotropic smectic A_d systems, e.g. the 4-*n*-alkyl-4′-cyanobiphenyls. An alternative suggestion was made for the structure of the thermotropic phase where the aliphatic chains are interdigitated and placed towards the centre of the layers, and the sugar moieties self-assemble in the outer regions of the bilayers [5]. This second model of the bilayer structure more appropriately resembles that of a cell membrane.

Subsequently, many studies were performed on liquid crystalline carbohydrates and related materials; however, the majority of the studies undertaken involved the investigation of substituted cyclic furanose and pyranose systems. Acyclic sugars on the other hand are underrepresented in the carbohydrate family of liquid crystals, especially taking into account the fact that they tend to be incorporated into the poly-ol genus. Nevertheless, for most of the mono-substituted acyclic systems investigated, e.g. structures **I** and **II** in figure 1, only smectic A* phases have been found to occur [6, 7]. Di-substituted systems, however, have been shown to exhibit more exotic phase behaviour; for example, Crystal B* phases [8] and columnar modifications (structure **III**, figure 1) have been found [9]. Moreover, as the degree of alkyl substitution is increased, it is apparent that columnar phases are preferred over calamitic structures [10].

Thus, this article is concerned with a systematic and fundamental investigation into the effects of the linking group (positioned between the sugar unit and the aliphatic chain in mono-substituted systems) on the liquid

*Author for correspondence.

0267–8292/97 $12·00

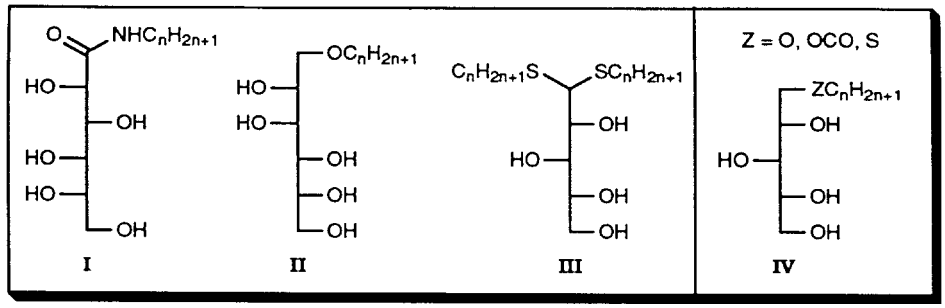

Figure 1. General structures of some acyclic carbohydrate liquid crystals.

crystalline properties of acyclic systems. As earlier investigations described aliphatic substituted tetrols as being liquid crystalline in nature, but of undefined phase type [11], we chose to study the mesomorphic behaviour of alkyl substituted xylitols where the aliphatic chain is attached to the xylitol moiety via ether, ester or thioether linkages respectively, see structure **IV** in figure 1.

Apart from our fundamental interest in the mesomorphic behaviour of these materials, the compounds also have practical uses as surfactants and non-ionic detergents. In addition, their abilities to self-organise and assemble can give insights into the structures and stabilities of membranes.

2. Experimental

2.1. *General synthetic procedures*

Aliphatic derivatives of xylitol (structure **IV**) were prepared following the general synthetic pathway depicted in the Scheme. The diacetal substrate, 1,2: 3,4-di-*O*-isopropylidene-D,L-xylitol, **1**, was prepared using the method reported by Regnaut [12]. The diacetal, **1**, was subsequently derivatized via different routes for the three families of materials. For the ether derivatives, compounds of general structure **3**, the diacetal was directly alkylated with various *n*-bromoalkanes in the presence of potassium hydroxide (step (i)). The esters, **4**, were prepared by reaction of the diacetal, **1**, with various acid chlorides in the presence of triethylamine (TEA) (step (ii)). Thioetherification of the diacetal to give compounds of structure **5** was achieved by first making the tosylate **2** (step (iii)), and then subjecting this to reaction with suitable thiols in the presence of potassium hydroxide (step (iv)). The conditions for the deacetalization of **3**, **4**, and **5** (step (v)) were selected with a view to obtaining simultaneously the desired products **9**, **10** and **11** and the corresponding monoacetalated compounds **6**, **7**, and **8**. The monoacetalated compounds are found not to be mesomorphic, but nevertheless they provide a new range of surfactants for other applications.

2.2 *Characterization of materials and measurement of physical properties*

All chemical reactions were monitored by either reverse phase HPLC (Waters 721) or GPC (Girdel)

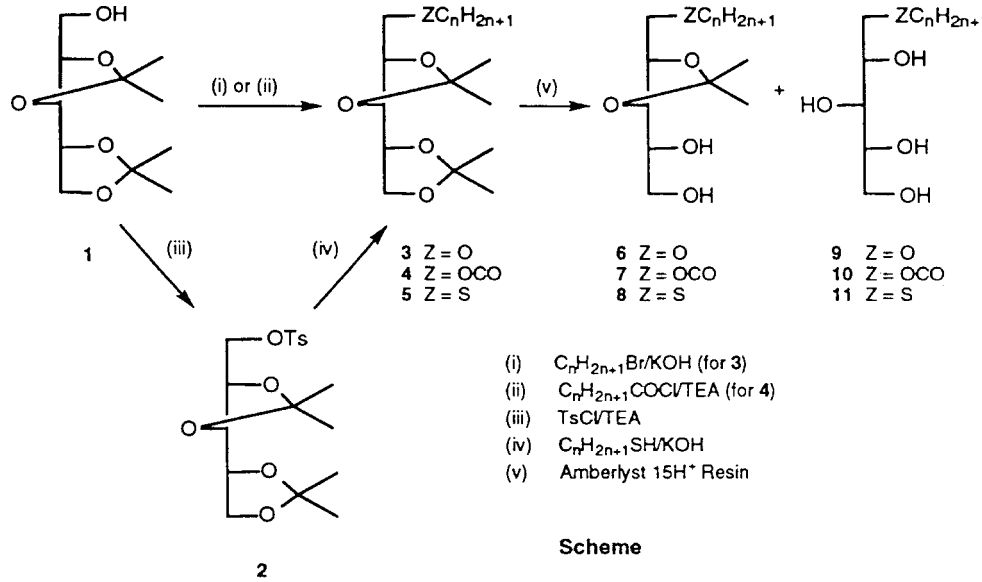

Scheme. Synthesis of materials.

chromatography. Reverse phase HPLC was carried out using either RP-18 (Merck) or PN 27–196 (Waters) columns, whereas GPC was performed using either OVE 17 or SE 30 columns. Purification of the final products was achieved by gradient column chromatography over silica gel (60 mesh, Matrex) using a mixture of hexane–acetone as the eluent (in each case the ratio of silica gel to product mixture to be purified was 30:1). The purities of the final compounds were determined by chromatographic, spectroscopic, and elemental analyses. The structures of all starting reagents, intermediates and final products, were determined by a combination of spectroscopic methods; for example, NMR spectra were recorded using a Bruker WP-300 spectrometer for solutions in $CDCl_3$ or C_5D_5N (tetramethylsilane was used as the internal standard). The melting point of each product was determined using an electrothermal automatic apparatus (the results reported are uncorrected).

Phase identifications and determination of phase transition temperatures were carried out, concomitantly, by thermal polarized light microscopy using either a Zeiss Universal or a Leitz Laborlux 12 Pol polarizing transmitted light microscope equipped with a Mettler FP82 microfurnace in conjunction with an FP80 Central Processor. Photomicrographs were obtained using a Nikon POH polarizing light microscope equipped with a Nikon AFM camera. Homeotropic sample preparations suitable for phase characterization were prepared simply by using clean glass microscope slides (washed with water, acetone, water, concentrated nitric acid, water and dry acetone), whereas homogeneous defect textures were obtained by using nylon coated slides. Nylon coating of the slides ($\sim$200–300 Å thick) was performed by dipping clean slides into a solution of nylon (6/6) in formic acid (1% wt/vol). The nylon solution was allowed to drain off the slides over a period of 1 h, and then they were baked dry, free from solvent, in an oven at 100°C for a period of 3 h. For the purposes of phase identification some of the slides were not buffed, as is usual for preparing aligned samples, but instead they were used untreated so that many defects would be created when the liquid crystal formed on the surface of the slide on cooling from the liquid phase.

Differential scanning calorimetry was used to determine enthalpies of transition and to confirm the phase transition temperatures determined by optical microscopy. Differential scanning thermograms (scan rate $10° \text{ min}^{-1}$) were obtained using a Perkin Elmer DSC 7 PC system operating on UNIX software. The results obtained were standardized relative to indium (measured onset 156·68°C, ΔH 28·47 J g^{-1}, literature value [13] 156·60°C, ΔH 28·45 J g^{-1}).

Comparison of the transition temperatures determined by optical microscopy and differential scanning calorimetry shows some slight discrepancies. This is due to two factors; firstly, the two methods used separate instruments which are calibrated in different ways, and secondly, and more importantly, the carbohydrates tended to decompose slightly at elevated temperatures and at different rates depending on the rate of heating, the time spent at an elevated temperature and the nature of the supporting substrate, i.e. the materials decomposed more quickly in aluminium DSC pans than on glass microscope slides.

Classification of the mesophases of the products was achieved via binary phase diagrams which were constructed by determining the phase transition temperatures of individual binary mixtures of a test material mixed with a standard compound of known phase transition sequence. The binary mixtures were produced by weighing out each individual test material and a known standard material on a microscope slide and mixing them thoroughly while in their liquid states. The cooled samples were introduced into the microscope microfurnace and the phase transition temperatures and classification of phase type were assessed in the usual manner. Typically, when the test and standard materials were mixed on a microscope slide while in their liquid states, some decomposition occurred thereby resulting in lower transition temperatures. In all cases, recrystallization temperatures were not determined because the binary mixtures supercooled to room temperature in their liquid crystalline states. Investigations of the lyotropic phases were carried out at room temperature by simply allowing crystals of the test material to dissolve in water, thereby creating a concentration gradient which supported mesophase formation.

Molecular modelling studies were performed on a Silicon Graphics workstation (Indigo XS24, 4000) using the programs Quanta and CHARMm. Within CHARMm, the Adopted Basis Newton Raphson (ABNR) algorithm was used to locate the molecular conformation with the lowest potential energy. The minimization calculations were performed until the root mean square (RMS) force reached 4·184 kJ mol^{-1} Å^{-1}, which is close to the resolution limit. The RMS force is a direct measure of the tolerance applied to the energy gradient (i.e. the rate of change of potential energy with step number) during each cycle of minimization. The calculation was terminated if the average energy gradient was less than the specified value.

The results of the molecular mechanics calculations were generated using the programs QUANTA V 4.0 and CHARMm V22.2. The programs were developed and integrated by Molecular Simulations Inc. The modelling packages assume the molecules to be a collection of hard particles held together by elastic forces, in the gas phase, at absolute zero, in an ideal motionless state, and the force fields used are those described in CHARMm V 22.2.

2.3. *Synthesis of Materials*

2.3.1. *General procedure for the preparation of 1-*O*-n-alkyl-2,3:4,5-di-*O*-isopropylidene-D,L-xylitols, **3***

Finely powdered potassium hydroxide (2 equiv) and the appropriate bromoalkane (1·2 equiv) were added to a stirred solution of the diacetal **1** (1 equiv) in 4:1 toluene/Me_2SO (100 g l^{-1}) at room temperature. After 95% conversion, the mixture was filtered and the filtrate neutralized with saturated aq NH_4Cl. The organic phase was separated, washed with water (2 × 100 ml), dried (Na_2SO_4), and the solvent removed under reduced pressure. The desired products were isolated after purification by column chromatography.

2.3.2 *General procedure for the preparation of 1-*O*-n-acyl-2,3:4,5-di-*O*-isopropylidene-D,L-xylitols, **4***

To a stirred solution of dry diacetal **1** in anhydrous toluene (125 g l^{-1}) at room temperature, TEA (1·1 equiv) was added, followed by the appropriate acid chloride (1 equiv). After complete reaction, the mixture was filtered and the solvent removed under reduced pressure. The desired products (see table 1) were isolated after purification by column chromatography.

The acid chlorides used were commercially available except for decanoyl chloride which was prepared by reaction of thionyl chloride (1·2 equiv) on the corresponding acid (1 equiv) in dry toluene, in the presence of pyridine (1 equiv) at 110°C. After 24 h, the solvent was removed under reduced pressure until the volume of the mixture was reduced to 50% of its original size. The resulting concentrated solution was then used to esterify the diacetal **1**, as described above.

2.3.3. *General procedure for the preparation of 1-*S*-n-alkyl-1-thio-2,3:4,5-di-*O*-isopropylidene-D,L-xylitols, **5***

p-Toluenesulfonyl chloride (9 g, 1·1 equiv) dissolved in dry toluene (15 ml) was added at room temperature to a mixture of the diacetal **1** (10 g) and toluene-TEA (5:1, 35 ml). After 24 h the mixture was filtered and the solvent removed under reduced pressure. The crude product was recrystallized from a mixture of 5:1 hexane-acetone giving the pure tosylate, **2**, in 96% yield (m.p. 75°C). Thioetherification was achieved via the dropwise addition of a solution of the appropriate alkyl thiol (2 equiv) in toluene, at 50°C to a stirred solution of KOH (2 equiv) and **2** (1 equiv) in 4:1 toluene/Me_2SO (150 g l^{-1}). After 95% conversion, the mixture was filtered, and the filtrate neutralized with saturated aq NH_4Cl. The organic phase was separated, washed with water (2 × 100 ml), dried (Na_2SO_4), and the solvent removed under reduced pressure. The desired products were isolated after purification by column chromatography.

2.3.4 *General procedure for the deprotection of intermediates **3**, **4**, and **5***

Wet Amberlyst 15H^+ resin was added, at 50°C, to a stirred solution of intermediates **3**, **4** or **5** in 9:1 ethanol/water (125 g l^{-1}) (in each case the weight ratio of the resin to substrate was 4:1). The reaction was monitored by HPLC, and once 95% of the diacetalized precursors **3**, **4**, **5** had been consumed the mixture was filtered and the solvent removed under reduced pressure. The desired products were isolated after purification by column chromatography (see table 1). The structures of the final products were elucidated by ^{13}C and ^{1}H NMR spectroscopy (see tables 2 and 3, respectively). The conditions for the deprotection also allowed for the monoacetal derivatives, **6**, **7**, **8** to be isolated.

3. Results and Discussion

3.1. *Thermotropic liquid crystal properties*

3.1.1. *Transition Temperatures*

The transition temperatures were determined by thermal optical microscopy and differential scanning calorimetry (DSC). The results obtained by both methods are shown together in table 4, and the clearing points for all three series of compounds, as determined by thermal optical microscopy, are shown together in figure 2.

It can be seen from table 4 and figure 2 that the clearing points rise as a function of aliphatic chain length in a way similar to results found for other related liquid crystalline carbohydrate systems [4, 14]. When the aliphatic chain is increased to twelve carbon atoms in length, i.e. the dodecyl homologue, the clearing points stabilize and level off. It is interesting to note that the thioethers have higher clearing points in relation to the esters, which are in turn higher than those obtained for the ethers. These results indicate the following order of efficiency of the functional groups in stabilizing liquid crystal properties for aliphatic substituted polyols.

$$RS- > RCOO- > RO-$$

At short chain lengths this order of efficiency becomes more pronounced with the thioethers being much more stable than the esters or ethers (i.e. the thioethers have ~60°C higher clearing temperatures). At longer chain lengths the discrepancy between the clearing temperatures of the thioethers and the esters shrinks to virtually nil; conversely the ethers still lag behind but to a lesser degree (~30°C).

3.1.2. *Phase classification*

The mesophases exhibited by all three series of compounds were determined, by miscibility studies, to be of the same classification type. Classification was achieved in two ways; firstly from observations of the defect textures exhibited by the mesophase on cooling from

Table 1. Physicochemical and microanalytical data for 1-*Z*-*R*-D,L-xylitols.

Products *n*	Yield %	Formula	Calculated C	Calculated H	Found C	Found H
Ethers	(*Z* = O)					
5	51 (31)	$C_{10}H_{22}O_5$	54·05	9·91	54·11	10·01
6	76 (19)	$C_{11}H_{24}O_5$	55·91	10·24	55·92	10·55
7	71 (21)	$C_{12}H_{26}O_5$	57·57	10·47	57·52	10·60
8	60 (31)	$C_{13}H_{28}O_5$	59·06	10·67	59·10	10·45
9	33 (45)	$C_{14}H_{30}O_5$	60·40	10·86	60·30	10·87
10	64 (16)	$C_{15}H_{32}O_5$	61·61	11·03	61·31	11·17
11	50 (40)	$C_{16}H_{34}O_5$	62·71	11·18	62·65	11·47
12	57 (32)	$C_{17}H_{36}O_5$	63·71	11·32	63·51	11·21
14	59 (16)	$C_{19}H_{40}O_5$	65·48	11·57	65·51	11·81
16	30 (40)	$C_{21}H_{44}O_5$	66·98	11·78	67·17	11·91
Esters	(*Z* = OCO)					
5	52 (34)	$C_{11}H_{22}O_6$	52·78	08·86	52·69	8·92
6	48 (42)	$C_{12}H_{24}O_6$	54·53	9·15	54·32	9·29
7	59 (30)	$C_{13}H_{26}O_6$	56·14	9·41	56·09	9·70
8	41 (50)	$C_{14}H_{28}O_6$	57·51	9·65	57·36	9·84
9	27 (57)	$C_{15}H_{30}O_6$	58·80	9·87	58·50	10·03
10	31 (51)	$C_{16}H_{32}O_6$	59·97	10·07	59·97	10·28
11	54 (27)	$C_{17}H_{34}O_6$	61·05	10·25	61·30	10·54
13	40 (43)	$C_{19}H_{38}O_6$	62·98	10·50	63·05	10·59
15	45 (46)	$C_{21}H_{42}O_6$	64·58	10·84	64·61	10·95
Thioethers	(*Z* = S)					
5	58 (31)	$C_{10}H_{22}O_4S$	50·42	9·24	50·54	9·30
6	58 (23)	$C_{11}H_{24}O_4S$	52·38	9·52	52·50	9·68
7	54 (34)	$C_{12}H_{26}O_4S$	54·14	9·77	54·28	9·91
8	61 (25)	$C_{13}H_{28}O_4S$	55·68	10·06	55·78	10·19
9	70 (26)	$C_{14}H_{30}O_4S$	57·14	10·20	57·25	10·31
10	47 (32)	$C_{15}H_{32}O_4S$	58·40	10·45	58·39	10·80
11	51 (31)	$C_{16}H_{34}O_4S$	59·63	10·56	59·71	10·80
12	70 (15)	$C_{17}H_{36}O_4S$	60·67	10·78	60·71	11·11
14	55 (40)	$C_{19}H_{40}O_4S$	62·59	11·06	62·69	11·46
16	60 (33)	$C_{21}H_{44}O_4S$	64·24	11·29	64·20	11·40

the isotropic liquid, and secondly through miscibility studies with standard materials.

The defect textures exhibited by the mesophase fall into three categories. On untreated clean glass substrates the compounds exhibited focal-conic, oily streak and homeotropic defect textures, see figure 3. On glass substrates treated with aligning agents, such as nylon, the materials showed focal-conic defects characterized by their elliptical and hyperbolic lines of optical discontinuity. In this case the focal-conic domains were found to be disordered in the plane of the glass even when the substrate had been buffed (buffing usually breaks the degeneracy in the plane). These observations indicate that the alignment of the focal-conic domains is a function of the interaction of the hydroxyl groups of the xylitols with the substrate surface. Many hydrogen bonding interactions can occur per molecule and hence the resulting specimen is disordered in the plane of the sample. Nevertheless, the presence of focal-conic defects and homeotropic alignment in variously treated specimens is indicative of the presence of a smectic A phase.

In addition, since the molecules are chiral, the specimens were examined for the formation of helical macrostructures, e.g. banding in the focal-conic domains, rotation of plane polarized light and selective reflection of light; however, none of these properties were found. Thus, the materials do not exhibit the twisted form of the smectic A phase, i.e. the twist grain boundary phase. These results classify the phase as being smectic A* in type.

Miscibility studies with a variety of related standardized carbohydrate liquid crystals were found to confirm the above hypothesis. For example, all the dodecyl substituted xylitols (thioether, ester and ether) were found to be independently miscible with the smectic A* phase of *n*-octyl 1-*O*-*β*-D-glucopyranoside [4].

Thus, the phase exhibited by all three sets of compounds is, not surprisingly, found to be smectic A* with a structure which might be expected [5] to resemble

Table 2. ^{13}C NMR chemical shifts of 1-*Z*-*R*-D,L-xylitol type **9**, **10**, **11** compounds in C_5D_5N. $\delta = 32{\cdot}-32{\cdot}5$ in all cases.

Products *n*	Xylitol moiety					Ester	Alkyl chain	
	C_1	C_2	C_3	C_4	C_5	–O–CO–	ZCH_2	ZCH_2CH_2
Ethers								
5	73·9	72·7	72·5	74·8	64·9		71·9	14·5
6	73·9	72·6	72·5	74·7	64·8		72·0	14·5
7	73·4	72·7	72·5	74·8	74·8		72·0	14·6
8	73·9	72·6	72·6	72·7	64·9		72·0	14·5
9	73·9	72·7	72·6	74·7	64·9		72·0	14·6
10	74·0	72·7	72·6	74·8	64·9		72·0	14·6
11	73·9	72·6	72·6	74·7	64·8		72·1	14·6
12	74·0	72·6	72·6	74·7	64·9		72·1	14·6
14	74·0	72·7	72·6	74·7	64·9		72·0	14·6
16	73·9	72·7	72·6	74·7	64·9		72·0	14·6
Esters								
5	67·3	71·7	74·3	72·6	64·7	174·0	34·8	14·4
6	67·2	71·7	74·2	72·6	64·7	173·5	34·7	14·4
7	67·3	71·8	74·3	72·6	64·8	174·1	34·8	14·6
8	67·2	71·8	74·3	72·5	64·8	174·1	34·8	14·6
9	67·4	71·8	74·4	72·6	64·8	174·1	34·8	14·7
10	67·4	71·8	74·3	72·6	64·8	174·1	34·8	14·6
11	67·4	71·8	74·4	72·6	64·8	174·1	34·8	14·7
13	67·4	71·8	74·4	72·6	64·8	174·1	34·8	14·7
15	67·4	71·8	74·4	72·6	64·8	174·1	34·8	14·6
Thioethers								
5	37·1	73·6	75·0	73·4	64·9		33·3	14·5
6	37·1	73·6	75·0	73·4	64·9		33·3	14·5
7	37·2	73·6	75·0	73·4	64·9		33·3	14·6
8	37·2	73·6	74·9	73·4	64·9		33·4	14·5
9	37·1	73·6	75·0	73·4	64·9		33·3	14·6
10	37·1	73·6	75·0	73·4	64·9		33·3	14·6
11	37·1	73·6	74·8	73·4	64·9		33·4	14·7
12	37·1	73·5	74·8	73·3	64·8		33·3	14·5
14	37·1	73·6	74·9	73·3	64·9		33·3	14·6
16	37·0	73·8	75·0	73·2	74·7		33·2	14·5

that shown in figure 4. In this structure, the aliphatic chains in adjacent pairs of layers are expected to partially interdigitate. The degree of interdigitation can be determined by X-ray diffraction (currently the topic of other studies on these and related systems). The carbohydrate moieties are expected to arrange themselves on the peripheral surfaces of this bilayer structure, and thereby resemble a membrane. The mesophase could therefore be classified as an interdigitated bilayer structure, and as the stronger intermolecular interactions are at the interfaces of the bilayer ordering, the structure could be said to be inverted relative to that normally found for the smectic A phase where the strong interactions are more likely to be found within the layer [5]. This structure allows for very small traces of water to be positioned between the carbohydrate residues of adjacent bilayers, thereby allowing for easy formation of lyotropic phases.

The proposed structure for the mesophase is in keeping with structures reported for similar phases of carbohydrate liquid crystals, which would classify the mesophase as smectic A_d^*.

3.2. *Lyotropic liquid crystal properties*

The lyotropic properties of the materials were investigated via the addition of water to the materials at room temperature. A few crystals of each compound were placed on a microscope slide and covered with a coverslip. Water was then introduced via capillary action at the edge of the slip. The solvation and dissolution processes of the materials were then observed by polarized optical microscopy. The lyotropic phase observed in each of the series of xylitols was the lamellar phase. This phase was identified from its characteristic defect textures; see figure 5.

Table 3. ^{1}H NMR chemical shifts of 1–*Z*–*R*–D,L-xylitol type **9, 10, 11** compounds in C_5D_5N.

Products *n*	Xylitol moiety							Alkyl chain	
	H_{1a} (J_{1a-1b})	H_{1b} (J_{1a-2})	H_2 (J_{1b-2})	H_3 (J_{2-3})	H_4 (J_{3-4})	H_{5a} (J_{4-5a})	H_{5b} (J_{4-5b}; J_{5a-5b})	ZCH_2	$CH_{3\omega}$
Ethers									
5	4·03	3·95	4·58	4·41	4·51	5·233	4·29	3·46	0·77
	(9·6)	(6·4)	(5·2)	(3·4)	(3·6)	(5·3)	(6·3; 10·9)	(6·6)	(7·0)
6	4·02	3·97	4·56	4·39	4·50	4·33	4·28	3·37	0·78
	(9·6)	(6·3)	(5·1)	(3·1)	(3·5)	(4·0)	(5·5; 10·8)	(6·6)	(6·6)
7	4·04	3·96	4·58	4·41	4·52	4·34	4·30	3·48	0·80
	(9·7)	(6·3)	5·2)	(3·4)	(3·5)	(5·3)	(6·3; 10·9)	(6·6)	(6·8)
8	4·06	4·01	4·62	4·45	4·55	4·37	4·35	3·51	0·83
	(9·6)	(6·3)	(5·2)	(3·6)	(3·8)	(5·2)	(5·9; 10·1)	(6·6)	(6·8)
9	4·06	3·98	4·60	4·42	4·53	4·36	4·31	3·51	0·85
	(9·6)	(6·3)	(5·2)	(3·6)	(4·1)	(5·1)	(5·8; 10·8)	(6·6)	(6·6)
10	3·98	3·91	4·52	4·37	4·47	4·30	4·26	3·44	0·78
	(9·6)	(6·4)	(5·2)	(3·3)	(3·7)	(5·1)	(5·9; 10·8)	(6·6)	6·7)
11	4·00	3·93	4·55	4·36	4·47	4·30	4·25	3·46	0·80
	(9·6)	(6·3)	(5·2)	(3·5)	(4·5)	(5·5)	(5·6; 10·9)	(6·6)	(6·5)
12	4·01	3·43	4·57	4·37	4·47	4·29	4·28	3·47	0·81
	(9·6)	(6·3)	(5·3)	(3·5)	(3·8)	(4·7)	(5·2; 10·6)	(6·6)	(6·7)
14	4·01	3·92	4·55	4·36	4·48	4·29	4·26	3·45	0·80
	(9·6)	(6·2)	(5·1)	(3·5)	(3·8)	(5·2)	(5·9; 10·9)	(6·6)	(6·7)
16	3·94	3·91	4·52	4·34	4·45	4·27	4·25	3·41	0·80
	(9·6)	(6·3)	(5·2)	(3·6)	(3·8)	(5·8)	(4·9; 10·6)	(6·6)	(6·6)
Ethers									
5	4·84	4·80	4·68	4·41	4·56	4·39	4·31	2·26	0·74
	(11·1)	(6·8)	(4·7)	(3·4)	(3·6)	(6·9)	(5·5; 11·0)	(7·5)	(6·7)
6	4·83	4·79	4·67	4·38	4·55	4·33	4·29	2·29	0·78
	(11·1)	(7·0)	(4·7)	(3·4)	(3·7)	(5·2)	(6·0; 11·1)	(7·5)	(6·8)
7	4·9	4·85	4·73	4·44	4·57	4·37	4·32	2·30	0·80
	(11·0)	(6·9)	(4·7)	(3·8)	(3·9)	(5·3)	(6·0; 11·0)	(7·5)	(6·9)
8	4·87	4·85	4·71	4·43	4·58	4·37	4·34	2·33	0·84
	(11·1)	(7·6)	(4·1)	(3·8)	(3·7)	(5·5)	(6·0; 10·9)	(7·5)	(6·8)
9	4·85	4·81	4·68	4·39	4·55	4·34	4·30	2·31	0·83
	(11·0)	(7·1)	(4·7)	(3·6)	(3·9)	(5·3)	(5·5; 11·0)	(7·5)	(6·7)
10	4·84	4·79	4·66	4·38	4·52	4·37	4·33	2·27	0·81
	(11·0)	(7·1)	(4·6)	(3·6)	(3·7)	(5·5)	(5·6; 11·1)	(7·5)	(6·7)
11	4·86	4·81	4·69	4·41	4·55	4·36	4·30	2·32	0·86
	(10·9)	(6·7)	(4·9)	(3·7)	(3·8)	(5·5)	(5·9; 11·0)	(7·5)	(6·6)
13	4·85	4·81	4·68	4·40	4·54	4·35	4·30	2·32	0·86
	(11·1)	(4·7)	(7·2)	(3·6)	(3·7)	(5·3)	(5·9; 10·9)	(7·5)	(6·6)
15	4·86	4·82	4·69	4·41	4·55	4·36	4·31	2·32	0·86
	(11·1)	(7·2)	(4·3)	(3·5)	(3·6)	(5·4)	(6·0; 11·0)	(7·5)	(6·6)
Thioethers									
5	3·31	3·20	4·54	4·55	4·47	4·38	4·32	2·63	0·80
	(13·2)	(7·0)	(5·8)	(8·8)	(3·3)	(5·3)	(6·0; 10·9)	(7·4)	(7·1)
6	3·32	3·21	4·52	4·55	4·47	4·38	4·32	2·62	0·78
	(13·2)	(7·1)	(5·9)	(8·9)	(3·9)	(5·2)	(6·0; 11·0)	(7·3)	(6·8)
7	3·32	3·21	4·52	4·55	4·48	4·38	4·32	2·66	0·81
	(13·2)	(7·2)	(5·8)	(9·1)	(3·2)	(5·0)	(6·0; 11·0)	(7·4)	(6·4)
8	3·33	3·22	4·53	4·54	4·48	4·37	4·32	2·68	0·84
	(13·2)	(7·1)	(5·8)	(9·0)	(3·0)	(5·2)	(5·8; 10·9)	(7·4)	(6·7)
9	3·32	3·22	4·55	4·55	4·47	4·38	4·32	2·68	0·85
	(13·2)	(7·1)	(9·0)	(9·0)	(3·1)	(4·9)	(5·9; 11·0)	(7·3)	(6·2)
10	3·32	3·22	4·52	4·55	4·48	4·38	4·32	2·68	0·86
	(13·2)	(7·1)	(5·9)	(9·1)	(3·6)	(5·3)	5·9; 11·0)	(7·3)	(6·7)
11	3·31	3·21	4·54	4·54	4·45	4·35	4·31	2·69	0·89
	(13·2)	(7·1)	(9·1)	(9·1)	(3·5)	(5·1)	(5·9; 10·9)	(7·4)	(6·7)
12	3·33	3·22	4·53	4·54	4·47	4·37	4·32	2·71	0·89
	(13·2)	(7·1)	(5·8)	(9·0)	(3·0)	(4·6)	(5·6; 11·1)	(7·3)	(6·5)
14	3·31	3·20	4·53	4·52	4·46	4·36	4·30	2·67	0·86
	(13·2)	(7·1)	(5·8)	(9·0)	(3·6)	(4·9)	(5·7; 10·9)	(7·3)	(6·4)
16	3·22	3·23	4·58	4·57	4·51	4·37	4·32	2·69	0·81
	(13·3)	(6·8)	(6·3)	(8·7)	(3·4)	(5·3)	(5·7; 10·8)	(7·3)	(6·7)

Table 4. Transition temperatures (°C) determined by thermal optical microscopy (clearing temperatures in bold) and DSC Enthalpy results, ΔH, ($J\,g^{-1}$) determined by DSC shown in square brackets.

n	Ethers ($Z=0$)	Thioethers ($Z=S$)	Esters ($Z=OCO$)
5	**22·0** m.p. 36·2 [150·3][a] cl.pt. 20·5 [2·7]	**84·8** m.p. 62·6 [146·5][a] cl.pt. 83·5 [7·7]	**28·0** m.p. 50·8 [128·6][a] cl.pt. 27·5 [2·9]
6	**57·4** m.p. 21·4 [122·7][a] cl.pt. 49·3 [5·865]	**107·6** m.p. 56·7 [125·1][a] cl.pt. 105·8 [8·65]	**73·8** m.p. 56·8 [141·3] glass −25·4 cl.pt. 74·1 [3·84]
7	**80·3** m.p. 29·1 [118·5][a] cl.pt. 80·7 [6·6]	**123·4** cryst—cryst 2 16·5 [24·0] m.p. 63·7 [134·9][a] cl.pt. 121 [8·8]	**97·0** complex m.p. 71·2 [99·5] (three crystal phases) glass −14·3 cl.pt. 92·9 [4·46]
8	**101·8** m.p. 48·9 [117·2] glass −46·6 cl.pt. 98·0 [6·3]	**132·3** m.p. 49·9 [151·8][a] cl.pt. 128·7 [7·8]	**112·1** m.p. 53·3 [142·7] glass −14·0 cl.pt. 110·0 [6·4]
9	**107·2** m.p. 36·5 [131] glass −15·3 [15·3] cl.pt. 103·5 [5·58]	**136·0** m.p. 55·5 [160·3] rec −10·3 [22·4] cl.pt. 136·4 [7·8]	**124·9** m.p. 62·3 [145·6] rec −12·3 [30·1] cl.pt. 124·7 [5·46]
10	**113·2** m.p. 56·2 [171·4] rec −16·1 [50·3] cl.pt. 109·8 [5·4]	**141·8** m.p. 58·0 [153] rec 5·8 [150] cl.pt. 141·9 [3·97]	**130·4** m.p. 61·89 [154] rec 40·1 [4·8] cl.pt 132·3 [4]
11	**115·5** m.p. 48·8 [147·5] rec 3·8 [65·6] cl.pt. 112·6 [4·65]	**142·5** m.p. 62·5 [174·4] rec 21·8 [30·8] cl.pt. 141·2 [5·6]	**136·2** m.p. 69·5 [156·3] rec 22·7 [42·6] cl.pt. 133·1 [4·7]
12	**114·7** complex m.p. 43·6 [55·0] (four crystal phases) rec 40·9 [44·3]	**142·9** m.p. 66·7 [177] rec 30·0 [179] cl.pt. 139·3 [4·36]	—
13	—	—	**146·1** m.p. 75·0 [165·2] rec 39·1 [42·4] cl.pt. 146·1 [3·37]
14	**116·7** m.p. 68·9 [183·8] rec 41·6 [18·3] cryst 2—cryst 1 31·4 [22·2][b] cl.pt. 112·112·5 [2·1]	**143·6** m.p. 66·3 [185·7] rec 50·5 [46] cl-pt. 140·7 [3·05]	—
15	—	—	m.p. 75·0 [165·2] rec 54·9 [53·5] rec 54·9 [53·5] cl.pt. 141·0 [2·4]
16	**114·5** m.p. 75·4 [1062] rec 52·5 [54] cl.pt. 110·5 [1·7]	**146·0** complex m.p. 67·2 [148·9] rec 59·2 [133·5] cl.pt. 145·5 [0·7]	—

[a] No recrystallisation determined upon cooling by DSC to −50°C.
[b] Crystal to crystal transitions determined on cooling.

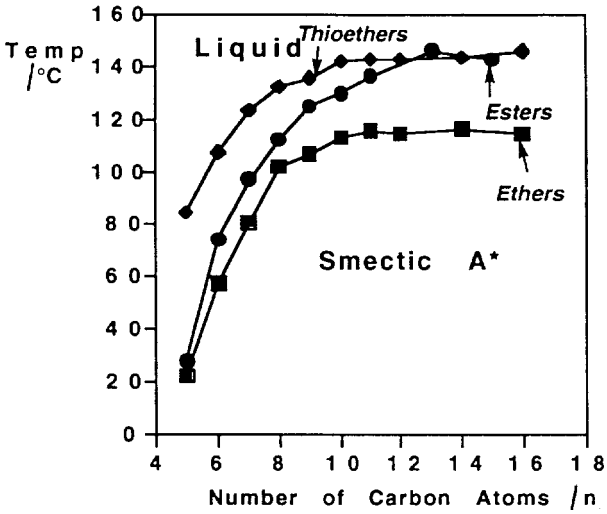

Figure 2. Clearing temperatures (°C) shown as a function of aliphatic chain length (n).

Comparisons of the results obtained for the three series can be drawn from table 5. It can be seen that the ethers more readily form lamellar phases than did either esters or thioethers. Only two examples of each of the ester and thioether series were found to exhibit lyotropic phases, whereas representatives were found for six ethers. These results tentatively provide a correlation for the efficiency of forming lyotropic phases for the three series as follows;

$$RO- > RS- \sim ROCO-$$

which is the reverse order with respect to the efficiency for thermotropic phases.

For all three series, the lamellar phase appears for the shorter homologues, but disappears at longer chain lengths. This effect is probably due to the decreasing solubilities of the materials as the aliphatic chain length is increased.

At room temperature, the ethers also show an interesting change-over from lyotropic to non-lyotropic properties with a change in phase behaviour for the nonyl to the undecyl homologues. Thus, the nonyl homologue exhibits a lamellar phase, whereas the decyl member is non-mesomorphic at room temperature and the undecyl homologue is again lamellar. It should be noted however, that these results are preliminary because no account has been taken of either the time for solvation of materials (i.e. the kinetic formation of mesophases was not investigated) or the temperature at which the lyotropic phases were formed (i.e. the construction of full temperature/concentration phase diagrams is out of the scope of this article, and therefore will be discussed in detail in a future report).

Table 5. Lyotropic phases at room temperature.

n	Ethers ($Z=0$)	Thioethers ($Z=S$)	Esters ($Z=OCO$)
5	lamellar	dissolves	dissolves
6	lamellar	lamellar	lamellar
7	lamellar	no LLCs	lamellar
8	lamellar	lamellar	no LLCs
9	lamellar	no LLCs	no LLCs
10	no LLCs	no LLCs	no LLCs
11	lamellar	no LLCs	no LLCs
12	no LLCs	no LLCs	–
13	–	–	no LLCs
14	no LLCs	no LLCs	–
15	–	–	no LLCs
16	no LLCs	no LLCs	–

3.3. *Molecular simulations*

Molecular simulations were used, in a pictorial way, to examine the spatial relationships between the atoms positioned in the regions of the linking groups in the three systems, and through simulations we were also capable of investigating how the motions of the aliphatic chain interfere with the ability of the sugar moiety to hydrogen bond in the neighbourhood of the linking

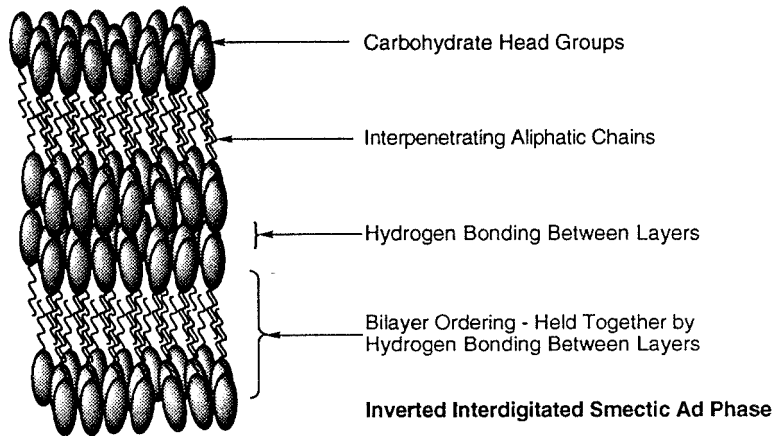

Figure 4. proposed structure of the thermotropic smectic A* phase formed by aliphatic substituted xylitols.

group of each family of compounds. The decyl homologues were selected for extensive simulation studies because for this chain length in all three series the isotropization temperatures start to level off. The geometrically optimized structures of the three decylxylitols studied are shown together in figure 6. Modelling was also performed on other members of each series, but no appreciable differences in the modelled structures could be discerned particularly in the neighbourhood of the linking group and sugar moiety as a function of aliphatic chain length.

Simulations of the three xylitol derivatives were also carried out at a temperature within the smectic A* phase. CHARMm dynamics were achieved, constraining only bonds containing hydrogens and using the parameter specified geometry. The molecular dynamics calculations were carried out in three stages: heating to 373 K, equilibrating the molecule at 373 K and simulating the motion of the molecule at 383 K, in the gas phase. The first two stages were necessary to prepare the model for the third simulation stage where CHARMm dynamics were performed for a simulated time of 6·4 ps, thereby generating 640 conformations. Average coordinates of these conformations produced time-average structures of the xylitol derivatives which were respectively found to be very similar to the conformations with the lowest potential energy.

The relative mobilities between the core and tail of the three xylitol derivatives were studied by allowing the substituent to rotate relative to the carbohydrate core. A conformational search around the C–*Z* bond (see below) was performed on the geometrically optimized structures. The search was done in a systematic way, using a 360° scan of the appropriate torsion angle with a 3° step sequence and, at each step, the grid torsion was defined and fixed artificially to prevent the stucture from returning to the original geometrically optimized structure. Each conformation generated in the stepwise rotation was geometrically optimized using a conjugate gradient algorithm and an energy gradient tolerance equal to 4·184 kJ mol^{-1} Å^{-1}.

It is possible to overlay the minimized rotational structures for each material in order to generate a model of the relative positions and energies of the different rotational conformers produced (see figures 7–9 for $Z =$ O, S, OCO, respectively). In these photographs the long axis of the xylitol moiety is perpendicular to the plane of the plate, and the freedom of motion of the aliphatic chain is shown as a disc centred on the xylitol unit. The colour coding of the disc depicts the relative degree of freedom of the decyl chain. The colour blue depicts a fairly unrestricted chain, whilst at the other extreme white represents conformationally disfavoured structures. It can be seen from figures 7 and 8 that the aliphatic chain in the thioether has more freedom of motion than that of the ether, which is a consequence of the small size of oxygen relative to sulphur. From this comparison, it appears that the thermotropic liquid crystal properties are stabilized when the motions of the aliphatic chain and the xylitol substrate are decoupled. The increased decoupling between the sugar unit and the aliphatic chain facilitates intermolecular hydrogen bonding interactions between the sugar moieties, which in turn stabilizes mesophase formation, i.e. the thioethers have the higher isotropization temperatures. Turning now to the ester derivatives, the ester linkage is more rigid than either the thioether or ether linkages, and because of this the aliphatic chain has a more restricted environment which, from the above arguments, should lower mesophase stability. However, the more rigid nature of the linking group effectively extends the length of the '*quasi*-core' or polar head-group, thereby stabilizing thermotropic properties. In addition, the carbonyl group of the ester can act as an extra point for hydrogen bonding interactions. Thus, we might expect the esters

Figure 3. The focal-conic, homeotropic and oily-streak defect textures of the thermotropic smectic A* phase of 1-*O*-*n*-dodecyl-D,L-xylitol.

Figure 5. The defect texture of the lamellar lyotropic phase of 1-*O*-*n*-hexyl-D,L-xylitol in water at room temperature.

Figure 6. The minimized energy conformations of the decyl homologues of the three series.

Figure 7. The stepwise rotations (about a total rotation of 360°) of the alkyl chain of 1-*O*-*n*-decyl-D,L-xylitol about the carbohydrate to aliphatic chain carbon–oxygen bond. The superimposed sugar moieties appear at the centre of the figure, whereas the superimposed rotational conformers of the aliphatic chain appear spread out as a disc. Blue shows regions where the chain has the most freedom to rotate, and white shows regions where it is restricted.

Figure 8. The stepwise rotations (about a total rotation of 360°) of the alkyl chain of 1-*S*-*n*-decyl-1-thio-D,L-xylitol about the carbohydrate to aliphatic chain carbon–sulphur bond. The superimposed sugar moieties appear at the centre of the figure, whereas the superimposed rotational conformers of the aliphatic chain appear spread out as a disc. Blue shows regions where the chain has the most freedom to rotate, and white shows regions where it is restricted.

Figure 9. The stepwise rotations (about a total rotation of 360°) of the alkyl chain of 1-*O*-*n*-undecanoyl-D,L-xylitol about the carbohydrate to aliphatic chain carbon–oxygen bond. The superimposed sugar moieties appear at the centre of the figure, whereas the superimposed rotational conformers of the aliphatic chain appear spread out as a disc. Blue shows regions where the chain has the most freedom to rotate, and white shows regions where it is restricted.

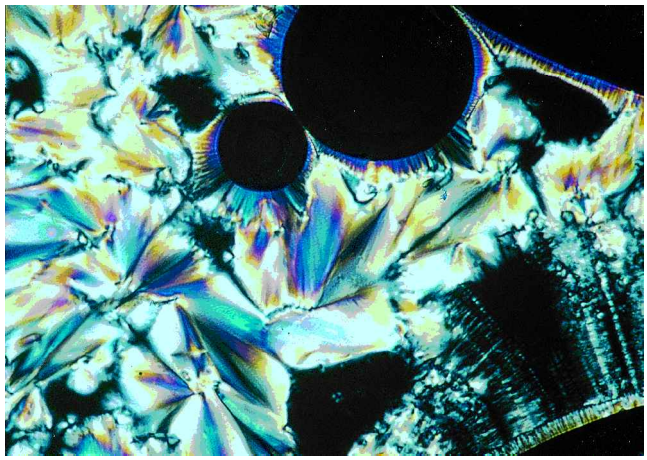

Figure 3

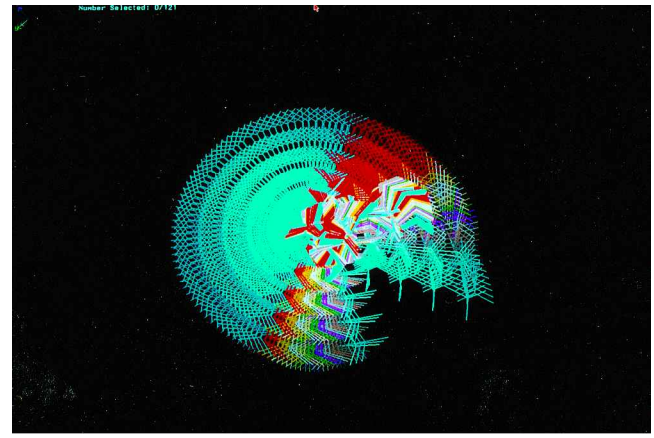

Figure 7

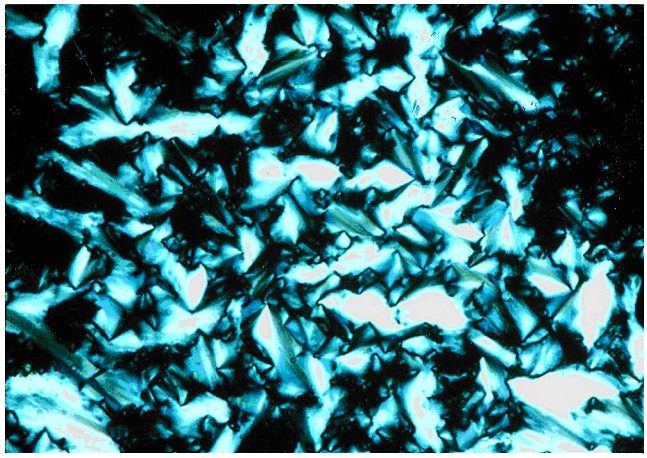

Figure 5

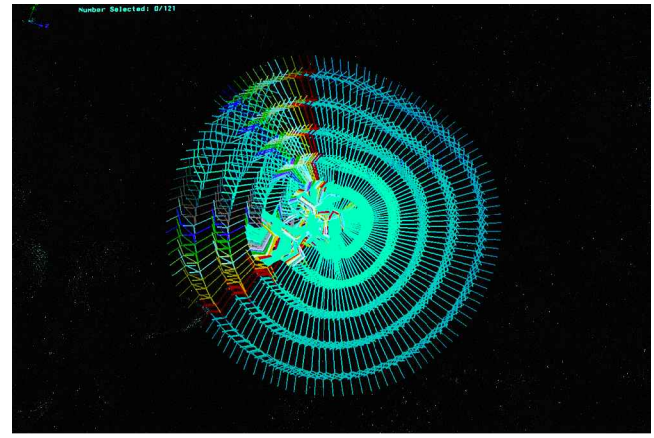

Figure 8

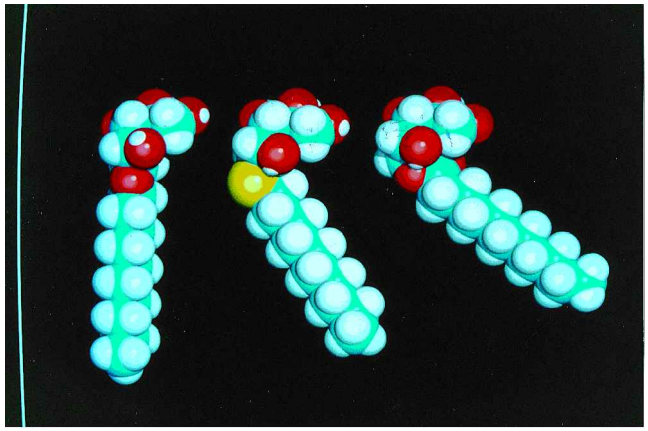

Figure 6

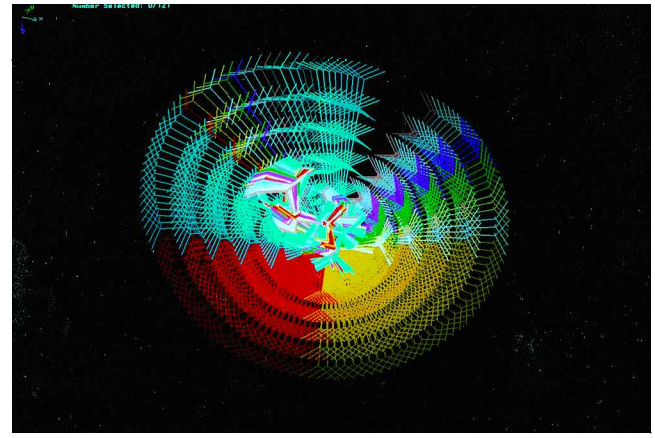

Figure 9

to have properties intermediate between those of ethers and thioethers.

In lyotropic systems, the reversal of the thermotropic stability sequence may be related to a reversal in the relative rôles of the dichotomous regions of the amphiphilic molecules. In the dry thermotropic state, the aliphatic chains can act as the liquid-like part of the phase with the sugar units giving the mesophase structure and rigidity. In comparison, in the lyotropic phase, the roles are reversed, the sugar moieties have the fluid-like interactions with water and the rigidity in this case is provided by the aliphatic chains which are excluded from the aqueous medium.

4. Summary

In this article we have comprehensively described the thermotropic and lyotropic liquid crystalline self-assembled structures of some substituted xylitols. We have developed structure–property correlations for the functional groups that link the aliphatic chain to the carbohydrate residue. We have also shown that the length of the aliphatic chain and its degree of rotational freedom strongly influence mesophase stability for both lyotropic and thermotropic phases. These results provide some of the first detailed structure–property correlations for carbohydrate liquid crystalline amphiphiles.

We would like to thank the EPSRC and the co-sponsored Alliance Programme of the British Council and the Ministere des Affaires Etrangeres, Direction de la Cooperation Scientifique et Technique for financial support of this research work.

References

[1] Jeffrey, G. A., and Bhattacharjee, S., 1983, *Carbohydr. Res.*, **115,** 53; Jeffrey, G. A, 1986, *Acc. chem. Res.*, **19,** 168; Jeffrey, G. A., and Wingert, L. M., 1992, *Liq. Cryst.*, **12,** 179 and references therein.

[2] Brown, G. H., and Wolken, J. J., 1979, in *Liquid Crystals and Biological Structures,* New York: Academic Press. van Doren, H. A., PhD thesis, 1989, Rijksuniversiteit Te Groningen; Chapman, D., Williams, R. M., and Ladbrooke, B. D., 1967, *Chem. Phys. Lipids*, **1,** 445.

[3] Noller, C. R., and Rockwell, W. C., 1938, *J. Am. chem. Soc.*, **60,** 2076; Garavito, R. M., and Rosenbusch, J. P., 1980, *J. Cell Biol.*, **86,** 327; Hall, C., Tiddy, G. J. T., and Pfannemüller, B., 1991, *Liq. Cryst.*, **9,** 527; Koynova, R. D., Tenchov, B. G., and Quinn, P. J., 1989, *Biochim. Biophys. Acta*, **980,** 377.

[4] Goodby, J. W., 1984, *Mol. Cryst. liq. Cryst.*, **110,** 205; Barrall, E., Grant, B., Oxsen, M., Samulski, E. T., Moews, P. C., Knox, J. R., Gaskill, R. R., and Haberfeld, J. L., 1979, *Org. Coat. Plast. Chem.*, **40,** 67.

[5] Van Doren, H. A., and Wingert, L. M., 1991, *Mol. Cryst. liq. Cryst.*, **198,** 381; Jeffrey, G. A., 1990, *Ibid*, **185,** 209.

[6] Pfannemüller, B., Welte, W., Chin, E., and Goodby, J. W., 1986, *Liq. Cryst.*, **1,** 357.

[7] Dahlhoff, W. V., 1989, *Z. Naturforsch.*, **44b,** 1105.

[8] Van Doren, H. A., and Goodby, J. W., unpublished results.

[9] Eckert, A., Kohne, B., and Praefcke K., 1988, *Z. Naturforsch.*, **43b,** 878.

[10] Prade, H., Miethchen, R., and Vill, V., 1995, *J. prakt. Chem.*, **337,** 427 and references therein.

[11] Kjaer, A., Kjaer, D., and Skrydstrup, 1986, *Tetrahedr.*, **42,** 1439

[12] Regnaut, I., Ronco, G., and Villa, P., 1989, FR Pat. No. 15995, Générale Sucrière.

[13] *CRC Handbook of Physics and Chemistry*, edited by R.C. Priest (Boca Raton: CRC Press) 68th Edition, 1988.

[14] Kohne, B., Praefcke, K., Stephan, W., and Marquardt, P., 1986, *Sep. Chimia*, **40,** 248; Kohne, B., Marquardt, P., Praefcke, K., Psaras, P., and Stephan W., 1987, *ibid.*, **41,** 63; Kohne, B., and Praefcke, K., 1986, *Z. Naturforsch.*, **41b,** 1036; Kohne, B., Praefcke, K., Stephan, W., and Nürnberg, P., 1985, *ibid.*, **40b,** 981; Kohne, B., Marquardt, P., Praefcke, K., Psaras P., and Stephan, W., 1987, *ibid.*, **42b,** 628.